Emergence of Sinai Physics in the stochastic motion of passive and active particles

Dekel Shapira and Doron Cohen

Department of Physics, Ben-Gurion University of the Negev, Beer-Sheva 84105, Israel

Abstract. A particle that is immersed in a uniform temperature bath performs Brownian diffusion, as discussed by Einstein. But Sinai has realized that in a "random environment" the diffusion is suppressed. Follow-up works have pointed out that in the presence of bias f there are delocalization and sliding transitions, with threshold value f_c that depends on the disorder strength. We discuss in a critical way the emergence of Sinai physics for both passive and active Brownian particles. Tight-binding and Fokker-Planck versions of the model are addressed on equal footing. We assume that the transition rates between sites are enhanced either due to a driving mechanism or due to self-propulsion mechanism that are induced by an irradiation source. Consequently, counter intuitively, the dynamics becomes sub-diffusive and the relaxation modes become over-damped. For a finite system, spontaneous delocalization may arise, due to residual bias that is induced by the irradiation.

1. Introduction

The most familiar type of stochastic motion is $random\ walk$ along a tight binding chain (lattice sites are labelled by n), where all the transition rates are identical. The dynamics is described by a rate equation

$$\dot{\boldsymbol{p}} = \boldsymbol{W}\boldsymbol{p} \tag{1}$$

where $\mathbf{p} = \{p_n\}$ are the probabilities to find the particle in any of the sites, and \mathbf{W} is a tridiagonal matrix whose off-diagonal elements are the transition rates. In the continuum limit the dynamics is described by a diffusion equation.

The question arises whether normal diffusion is affected by disorder. The simplest type of disorder arises if the rates w_n on each bond are random, aka bond-disorder or resistor-network-disorder. Hereafter we assume that the bond-disorder is weak, such that the probability to observe a disconnected chain is zero. Accordingly, for such type of disorder, the dynamics remains 'normal'.

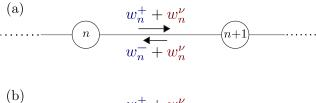
Sinai model.— Sinai had proposed to study a more general model that has been termed random walk in random environment [1]. In this model the rates w_n^{\pm} for forward and backward transitions over the n-th bond are uncorrelated (instead of being equal). The stochastic field over the n-th bond is defined thorough the ratio, namely, $w_n^+/w_n^- = \exp[\mathcal{E}_n]$. Assuming that the \mathcal{E}_n are uncorrelated, it follows that in the absence of bias $(\langle \mathcal{E} \rangle = 0)$ the spatial spreading is sub-diffusive $(x \sim \ln^2(t))$ rather than diffusive $(x \sim \sqrt{t})$.

Sliding transition.— Subsequent works by Derrida and followers [2, 3, 4] have considered the effect of non zero bias $f \equiv \langle \mathcal{E} \rangle > 0$. The existence of a critical bias f_c has been highlighted, such that for $f < f_c$ the drift velocity vanishes, while for $f > f_c$ it becomes finite. This has been termed sliding transition. We note that Sinai has assumed that the \mathcal{E}_n are strictly uncorrelated. The implications of long range correlations have been studied as well in [5], highlighting a crossover between Ohmic, Creep, and Sinai regimes. It is only in the latter case (of effectively uncorrelated disorder), that one observes a sharp sliding transition.

Delocalization transition.— From a completely different perspective Hatano, Nelson and followers [6, 7, 8, 9, 10, 11] have considered the delocalization transition for non-Hermitian Hamiltonians. In the present context the role of the non-Hermitian Hamiltonian is taken by the real non-symmetric (and hence non-Hermitian) matrix \boldsymbol{W} that conserves probability ($\sum p_n = 1$). The details of the delocalization scenario in the stochastic context have been discussed in [12, 13]. Here we are talking about the relaxation modes $\psi^{(r)}$ that are associated with eigenvalues λ_r of a finite length ring. They are determined by the equation

$$\mathbf{W}\psi = -\lambda\psi \tag{2}$$

The trivial eigenvalue $\lambda_0 = 0$ corresponds to the steady state. Delocalization is indicated by complex eigenvalues. For large enough f the eigenvalues at the vicinity of $\lambda = 0$ become complex, which implies under-damped relaxation. The term 'delocalization'



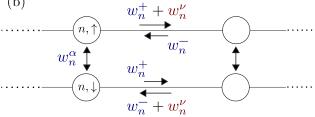


Figure 1. (a) Passive particle on a chain, sites labelled by n. The transition rates w_n^{\pm} are induced by a bath that has temperature T. Extra transitions w_n^{ν} are induced by a driving source. (b) Active particle on a chain. Such particle has an extra degree of freedom $s=\uparrow,\downarrow$ that indicates its orientation. The bath induced rates are w_n^{\pm} in the n coordinate. The flipping rate in the s-coordinate is w_n^{α} . Extra transitions w_n^{ν} are induced by the propulsion.

reflects the insight that for a ring geometry under-damped relaxation towards the steadystate is associated with complex-valued relaxation-modes that are extended over the ring. It has been emphasized in [12] that the threshold field for this *finite-size-system* transition is smaller than the f_c that is estimated for sliding along an infinite chain.

1.1. The Physics behind Sinai Physics

The model of Sinai is rather artificial. One wonders what are the physical assumptions that imply the emergence of the sliding and the delocalization transitions. The stochastic filed is defined via $w_n^+/w_n^- = \exp[\mathcal{E}_n]$. For a chain that is coupled to a single bath that has temperature T the stochastic field is

$$\mathcal{E}_n[\text{single bath, no driving}] = \frac{V_n - V_{n+1}}{T}$$
 (3)

where V_n is the on-site potential. This field exhibits telescopic correlations, that reflect the bounded energy landscape of V_n , while Sinai model assumes uncorrelated stochastic field whose potential features activation barriers of height $\propto \sqrt{L}$ for segments of length L.

The emergence of Sinai Physics necessitates a mechanism that breaks the telescopic correlations of the stochastic field. One simple option is to assume non-uniform temperature such that $\mathcal{E}_n = [V_n - V_{n+1}]/T_n$, with uncorrelated T_n on each bond. In the present work we would like to consider more interesting setups that are illustrated in Fig.1. In both setups the system is a tight binding chain immersed in a bath that has a uniform temperature. In the absence of "irradiation" the particle performs a diffusive motion. With "irradiation" the transition rates between sites are enhanced. The counter-intuitive expectation, based on Sinai's argument, is to witness sub-diffusion

instead of diffusion. To get an insight for this puzzling expectation, note that on short times one is likely to witness an enhanced spreading rate. But we focus on long times. Then it is important to notice that it is not the *rates* of transitions but the *topography* of the stochastic potential that matters (for argumentation purpose note that this topography is not affected if all the rates are multiplied by the same large factor). Due to the irradiation, the topography of the stochastic potential features an ever growing activation barriers that suppress the long time spreading, which is the essence of Sinai Physics.

1.2. Paradigms for anomalous transport

There are of course different paradigms for anomalous transport. But we focus here on what we call "Sinai Physics". For sake of clarity, following Sinai, we consider weak disorder: not only that the probability to observe a disconnected bond is zero, but furthermore it is assumed (for sake of argumentation) that all the rates are comparable. In particular it is implied that $\mathcal{E}_n \ll 1$. This weak disorder assumption allows in a later stage to adopt a very convenient continuum-limit Fokker-Planck approximation for the dynamics.

The model of Sinai is strictly one-dimensional (1D). Merely from a geometrical point of view, local barriers can block transport. In more than 1D one generically encounters rugged landscape that features ponds and outlets, see e.g. discussion in [14]. Note however that signatures of Sinai Physics may arise for the dynamics along the infinite cluster in the vicinity of a percolation threshold.

It is important to appreciate that "Sinai Physics" is not the only mechanism for anomalous transport. Increasing the activity in conjunction with quenched disorder can lead to counter-intuitive results that are not necessarily related to Sinai Physics. Particle-particle interactions in combination with quenched disorder generically produce such effects. Ref.[15] has considered the run-and-tumble dynamics of disks that move in a disordered array of fixed obstacles. Such system exhibits non-monotonic transport response due to crowding clogging and jamming; the motion is almost blocked and proceed in the form of avalanches [16]; and under bias might exhibit negative differential mobility [17]. This type of dynamics can be demonstrated also for a lattice version [18, 19].

1.3. Scope of this paper

We consider two models for which Sinai Physics is likely to emerge. The models are illustrated in Fig.1. In the absence of "irradiation" the particle performs transitions that are dictated by Eq.(3). In the presence of "irradiation" the rates are enhanced. Specifically:

• Passive-particle model.— In the model that is described by Fig. 1a, the chain is irradiated by a high-temperature source. The term 'irradiation' does not have to

be taken literally, it is just a convenient way to describe the effect of a second bath, that is regarded as a driving-source. For an infinite-temperature source the transition rates become $w_n^{\pm} + w_n^{\nu}$. The extra rates w_n^{ν} that are induced by the irradiation are not biased to any direction.

• Active-particle model.— In the model that is described by Fig.1b, the irradiation induces self-propulsion. What we have in mind are Janus particles [20, 21, 22, 23] immersed in a solution (those spherical nano-particles are coated at their two hemispheres with a different materials). Using a tight-binding language, the self-propulsion is incorporated as follows: a w_n^{ν} term is added to the w_n^+ rate (to the w_n^- rate) if the particle faces the forward (backward) direction respectively. The particle flips orientation randomly with rate w_n^{α} .

We would like to treat both models on equal footing. In both models the intensity of the irradiation is denoted by ν . It is important to emphasize that the irradiation by itself does not create any bias (the rates are enhanced "equally" in both directions). Given ν we can add an external bias f, and ask whether a threshold value f_c emerges.

Open issues.— The emergence of Sinai Physics due to driving or propulsion is somewhat counter-intuitive. In quasi-equilibrium conditions, under the influence of a bath that has uniform temperature, the system feature normal diffusion, while the extra transitions due to driving or propulsion mechanism lead to sub-diffusion and localization. This (and similar) counter-intuitive statements have been pointed out in some previous works in a way that was either blurred due to emphasis on related themes [24, 25], or restricted to non-Brownian "run-and-tumble particle" scenario [26, 27] where the motion is frozen in the absence of propulsion (rather than diffusive). Also the strong relation between tight-binding chains and their continuum limit version has not been adequately clarified. In this context one should be aware that the standard theory of Sinai physics does not apply for non-equilibrium quasi-one-dimensional chains. This means that an active-particle, unlike passive-particle, is not a-priori compatible with Sinai model.

The experimental aspect has to be addressed carefully. One arena where 1D stochastic physics can be tested is in the context of Brownian Motors [28]. The major signatures of Sinai physics is sub-diffusive spreading. In is common to determine the dependence of the sub-diffusion exponent on the bias, and to look for a sliding transition. A second arena for testing stochastic physics is inspired by experiments that we mentioned with Janus particles [20, 21, 22, 23]. We claim that the realization of an appropriate setup for demonstrating Sinai Physics in this context is challenging (see concluding section). In such system it might be feasible not only to characterize the spreading, but also to probe the relaxation modes [25], looking for a crossover from over-damped to under-damped relaxation (delocalization transition).

Outline.— In Sec.(2) we review the basic notion that are used in order to describe stochastic dynamics that is generated by a rate equation. In Sec.(3) we explain the essence of Sinai physics, and present some numerical results to motivate the later analysis. In particular we make the distinction between the non-equilibrium physics

of active-particle and the quasi-equilibrium physics of passive-particle. In Sec. (4) and Sec. (5) we provide detailed analysis for passive-particle, both for its tight-binding version, and for its Fokker-Plank continuum limit. The dependence of f_c on the driving intensity ν is found. In Sec. (6) we consider the emergence of Sinai Physics for a Brownian active particle: without propulsion the particle performs diffusion, while with propulsion it becomes sub-diffusive. In Sec. (7) we focus on the delocalization perspective. In particular we discuss the question whether for a finite size sample a residual affinity can induce spontaneous delocalization. Finally, in Sec. (8) we summarize our findings, and critically discuss their relevance for experiments with Janus particles.

2. Rate equations

In this section we summarize the terminology that is used in order to mathematically-characterize a rate-equation $\dot{\boldsymbol{p}} = \boldsymbol{W}\boldsymbol{p}$ that is defined over a network. In particular we define what are affinities, and what does it mean 'detailed balance', as opposed to genuine non-equilibrium conditions. Subsequently we focus on (infinite) *Chain* and (finite) *Ring* geometries.

Stochastic field.— Consider a system that is described by a rate equation. From a mathematical point of view we can regard the set of sites as nodes of a network, labeled by some index n. On each bond of the network we have forward and backward transition rates, and the stochastic field is defined as

$$\mathcal{E}_{nm} \equiv \ln \left[\frac{w_{mn}}{w_{nm}} \right] \tag{4}$$

If the rates are due to a bath that has a different temperatures T_{nm} on each bond, we get

$$\mathcal{E}_{nm} = \left[\frac{V_n - V_m}{T_{nm}} \right] \tag{5}$$

The circulations of \mathcal{E} are called affinities. Using obvious continuum-limit notations the affinity of a closed loop is

$$\Phi \equiv \oint \mathcal{E}(x)dx \tag{6}$$

For uniform temperature T any circulation of \mathcal{E} is zero, meaning that the field is conservative. We than say that we have detailed-balanced conditions that reflect equilibrium. More generally, even if the temperature is not uniform, we might have a conservative stochastic field. In particular, this is always the case for a one-dimensional chain with only near-neighbor transitions, simply because such geometry has trivial topology with no circulations.

Steady State.— Whenever we have detailed-balanced (absence of non-zero circulations) the stochastic field is conservative, and then we can define a stochastic potential U such that

$$\mathcal{E}_{nm} = U_n - U_m \tag{7}$$

Consequently, if the system is of finite-size, it relaxes towards a canonical steady state (SS):

$$p_n^{\rm SS} \propto e^{-U_n}$$
 (8)

On the other hand, if the stochastic field is not conservative (absence of detailed balance due to non-zero circulations), we cannot derive it from a potential U, and therefore the steady state is not canonical. Such non-equilibrium steady state (NESS) features non-zero currents.

Passive particle.— Consider the passive particle of Fig. 1(a). For a *Chain* of length L one observes that due to the trivial topology (no circulations) the system is detailed-balanced. This holds even if each of the bonds has a different temperature. Adding a driving source, the potential U is still well defined. What we call bias refers to the average value of the stochastic field:

$$f \equiv \frac{1}{L} \sum_{n} \mathcal{E}_{n} \tag{9}$$

For a ring of length L, non-zero bias implies non zero affinity $\Phi = fL$. For zero affinity $(\Phi = 0)$ the potential U along the ring is well defined, and the NESS is canonical. For a biased ring the NESS features a non-zero current. An explicit expression that generalizes Eq.(8) can be found in Appendix A.

Active particle.— Considering the active particle of Fig.1(b), one observes that there is non-zero circulation in each cell of the network. The nodes of the network are labeled by the coordinates (n, s), where n is the site index, and $s = \uparrow, \downarrow$ indicates the forward/backward orientation of the particle. The circulation around a unit cell reflects the propulsion. We are dealing here with a genuine non-equilibrium system. It is not possible to define a stochastic potential U. An exact explicit expression that generalizes Eq.(8) cannot be found, though approximations can be attempted in limiting cases, e.g. see Appendix B.

3. The emergence of Sinai Physics

In this section we clarify how 'Sinai Physics' emerges in the context of an (infinite) Chain and in the context of a (finite) Ring. In particular we illuminate subtleties that are related to the identification of Sinai Physics for active particles.

Sinai physics for a passive particle.— Sinai Physics arises for the passive particle of Fig. 1(a) if the \mathcal{E}_n become effectively uncorrelated. What we mean by 'effectively uncorrelated' is that the stochastic potential U, unlike V, becomes unbounded such that $|U(x+r)-U(x)| \sim \sqrt{r}$. The simplest way to get an effectively uncorrelated potential is to consider hypothetical situation where each bond has a different temperature. Such type of disorder breaks the telescopic correlations of stochastic field Eq.(5). The integral over this field provided the stochastic potential of Eq.(7). This integral is formally like adding random variables, and therefore features \sqrt{L}

fluctuations over segments of length L. Those unbounded fluctuations are responsible for the sub-diffusive spreading that has been highlighted by Sinai and followers.

Sinai physics for an active particle.— The standard argument that has established the emergence of Sinai physics for a passive particle, fails for the active particle of Fig.1b. Namely, in the latter case it is impossible to define a stochastic potential U. Still we can argue that this quasi-one-dimensional system is similar to Sinai model, namely, it can be approximated by the same geometry as that of Fig.1a. We shall discuss 3 options: (1) Reduction to an effective Sinai model; (2) Inspection of the NESS; (3) Inspection of the spectrum. The first option would provide, at best, an approximation. We shall see that in practice it is quite limited, and not very satisfactory. Let us elaborate further on the two others options.

Inspection of the NESS.— One can argue that the failure to find a satisfactory reduction of a quasi-one-dimensional network to an effective single-channel Sinai-model is a technical issue. Maybe in principle it is always possible to find an effective-Sinai-model? Let us see what is the implication of such *conjecture*, and whether we can benefit from it. Assuming that the active particle indeed can be approximated, after coarse-graining, by an effective Sinai model, it follows that the NESS is canonical-like. Then it is possible to extract an effective stochastic potential via the NESS. Namely, assuming that the NESS is provided by Eq.(8) with an effective potential U_n , it follows that the effective field is:

$$\mathcal{E}_n^{\text{eff}} \equiv \ln \left[\frac{p_{n+1}^{\text{NESS}}}{p_n^{\text{NESS}}} \right]$$
 (10)

where $p_n = p_{n,\uparrow} + p_{n,\downarrow}$ is the probability to find the particle in site n. For the standard Sinai model the above definition leads to the trivial identification $\mathcal{E}_n^{\text{eff}} = \mathcal{E}_n = \ln(w_n^+/w_n^-)$. But for a quasi-one dimensional network, that does not satisfy the detailed-balance condition, there is no simple way to relate the effective field to the local rates. Still, from a practical point of view we can benefit from the above definition. Given \mathbf{W} , it is a rather easy task to find the NESS, and using Eq.(10) to deduce $\mathcal{E}_n^{\text{eff}}$. The effective stochastic potential U_n^{eff} is obtained by integrating over the field. From this effective potential we can deduce what is f_c . We will test numerically whether this conjecture-based prediction is valid.

Inspection of the Spectrum.— The question arises how to test predictions for f_c that are based on a coarse-graining approximation or on a conjecture regarding its feasibility. We ask for an approximation-free conjecture-independent way to determine f_c . To determine f_c numerically for the sliding transition is not practical (as explained below). Fortunately, Sinai physics can be detected via the delocalization transition that precedes the sliding transition. This option is extremely convenient numerically for the following reason: Numerical testing of the sliding transition is too tough, because it requires a large ensemble and proper finite-size-scaling procedure. The drift velocity v is zero for $f < f_c$ only if the $L \to \infty$ limit is taken, and an average over realizations is formally required. In contrast, the related delocalization transition is easy for detection. Considering a single realization of a ring that has a finite length L, one can

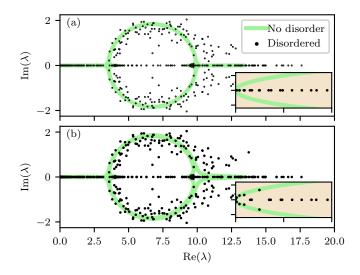


Figure 2. The relaxation spectrum for the active particle of Fig. 1b. The thick lines are $\lambda_{k,\pm}$ of the two bands via exact diagonalization of W for a non-disordered system. The dots are found via numerical diagonalization for a ring of length L=300. The unbiased transition rates are $w^{\beta}=1$, the propulsion rate is $\ln(w^{\nu})=1$, and the flipping rate is $w^{\alpha}=2$. The disorder parameters are $\sigma_{v}=1$ and $\sigma=0.1$, as defined after Eq.(24). Panels (a) and (b) are for $f=10^{-4}$ and $f=10^{-2}$, respectively, that are smaller and larger than f_{c} . The insets depict the spectrum at the vicinity of $\lambda=0$, with a zoom of factor $\times 10^{4}$ in (a) and $\times 10^{2}$ in (b) for the vertical axis, and $\times 3$ for the horizontal-axis. For a non disordered system the zoomed region can be approximated by Eq.(11) where $v \propto f$. With disorder the spectrum in the vicinity of $\lambda=0$ remains real for $f < f_{c}$, and indicates delocalization for $f > f_{c}$.

look for the threshold field that is required to get complex eigenvalues at the vicinity of $\lambda = 0$. For a clean ring, that has the simple geometry of Fig.1a, the eigenvalues become complex for any f > 0, namely,

$$\lambda_k \approx Dk^2 + ivk, \qquad k = \frac{2\pi}{L} \times \text{integer}$$
 (11)

where v is the drift velocity, and D is the diffusion coefficient. With disorder this approximation is valid only if both v and D are finite. This happens for a bias that exceeds the critical value that is calculated for the sliding transition. But a proper analysis [12] has clarified that the actual threshold for the delocalization transition precedes the estimated value for the sliding transition. We shall further discuss those thresholds in Sec.(7).

For the active particle of Fig.1b the delocalization transition is more subtle. Here complexity of an eigenmode does not imply that it is *extended* in space. The matrix W is not similar to an hermitian matrix even if the bias f is zero, since the hermiticity is spoiled by the propulsion. Complex eigenmodes can reside in localized loops of the network. Still, we can rationalize the association between the sliding transition and delocalization as follows. In the absence of disorder, and for zero propulsion, the spectrum is real and consists of two bands, see [25] and Appendix C. The lower band extends from $\lambda = 0$ up to twice the switching rate, where it start to overlap with the

second band. Complexity due to propulsion appears in the band-overlap region, and does not affect the $\lambda = 0$ region. (a detailed explanation of this point is provided at the end of Appendix C). It is therefore valid to claim that features of the spectrum at the vicinity of $\lambda = 0$ provide indication for the coarse grained dynamics of the spreading. We therefore expect a Sinai-type scenario. This expectation is supported by the demonstration in Fig.2.

4. Passive particle

In this section we consider the emergence of Sinai physics for the chain whose unit cell is sketched in Fig.1a. We treat an L site ring and a chain on equal footing. Accordingly we assume periodic boundary conditions, and label the sites by n modulo L, or by x in the continuum limit. The forward(+) and backward(-) transition rates between the nand n+1 sites are:

$$w_{n^{\pm}} = w_n^{\beta} e^{\pm \Delta_n/2T_n} + w_n^{\nu} \tag{12}$$

$$\equiv w_n^{\beta} \left[e^{\pm \Delta_n/2T_n} + \nu g_n \right]$$

$$\equiv w_n^{\beta} e^{\pm \mathcal{E}_n/2}$$
(13)

$$\equiv w_n^{\beta} e^{\pm \mathcal{E}_n/2} \tag{14}$$

The first term in Eq.(12) represents bath induced transitions between sites that have a potential difference $\Delta_n = -[V_{n+1} - V_n]$. The local bath temperature is T_n . The second term w_n^{ν} represent extra transitions that are controlled by an illumination source of intensity ν . The optional notation of Eq. (13) defines dimensionless coupling g_n . In the numerics we assume that thy have a log-normal distribution. It is convenient to normalize them such that $\langle \ln(g_n) \rangle = 0$, and thus the definition of the irradiation intensity ν is implied. Finally, the stochastic field on the n-th bond has been defined in accordance with Eq.(4), namely,

$$\mathcal{E}_n = \ln \left[\frac{w_{n^+}}{w_{n^-}} \right] \tag{15}$$

The high-temperature approximation can be written as

$$\mathcal{E}_n \approx \left(\frac{1}{1+\nu g_n}\right) \left[\frac{V_{n+1} - V_n}{T_n}\right] \tag{16}$$

$$\equiv -\beta_n[V_{n+1} - V_n] \tag{17}$$

where the β_n are defined via the last equality. The average stochastic field f has been defined in Eq. (9). If the only mechanism for transition is a bath with uniform temperature we get f=0. We can get $f\neq 0$ either due to non-uniform β_n , or by adding an external bias field, aka affinity (the former term is commonly used for a chain, while the latter is commonly used for a finite ring). The practical way to introduce bias f in a numerical illustration is to use the prescription

$$w_{n^{\pm}} \mapsto w_{n^{\pm}} \exp(\pm f/2)$$
 (18)

In accordance with this reasoning we define an L periodic stochastic potential U_n for zero bias, while for finite bias we write

$$\mathcal{E}_n \equiv f - [U_{n+1} - U_n] \tag{19}$$

The drift velocity.— Due to f one obtains NESS with non-zero current that has a drift velocity [2, 3, 4]

$$v_{\text{drift}} = (1 - e^{-fL}) \left[\frac{1}{L} \sum_{n=1}^{L} \frac{1}{w_{n+}} \sum_{r=0}^{L-1} e^{-fr + [U_n - U_{n-r}]} \right]^{-1}$$
 (20)

The infinite chain limit is formally obtained by setting $L = \infty$. In the absence of disorder one obtains an L-independent drift $v_{\text{drift}} = w_+ (1 - e^{-f}) = w_+ - w_-$, and for weak bias $v_{\text{drift}} = wf$, as expected. But if the stochastic field is disordered the drift velocity vanishes for $f < f_c$. The definition of the critical field f_c is implied by inspection of the sum in the square brackets: by definition the sum diverges for $f < f_c$.

Uncorrelated field.— Let us first remind how f_c is estimated for the standard Sinai-Derrida model, where the \mathcal{E}_n are assumed to be uncorrelated random variables. In the absence of bias (f=0) we define $\langle e^{-\mathcal{E}} \rangle \equiv e^{f_1}$. Then, in the presence of finite bias f we get

$$v_{\text{drift}} \approx \left[\frac{1}{L} \sum_{n=1}^{L} \frac{1}{w_{n+}} \sum_{r=0}^{L-1} e^{-(f-f_1)r} \right]^{-1}$$
 (21)

$$= \left\langle \frac{1}{w_{n+}} \right\rangle^{-1} \left[1 - e^{-(f-f_1)} \right] \tag{22}$$

where the latter equality holds if the geometric sum converges, i.e. for $f > f_1$. Accordingly one deduces that $f_c = f_1$. If the stochastic field has a Gaussian distribution we get $f_c = f_1 = (1/2) \text{Var}(\mathcal{E})$.

Correlated field.— In our case the \mathcal{E}_n are correlated, and not Gaussian distributed. We looks on the random variable $u = (U_{n+r} - U_n)$. It has zero average, and we assume that it is "small". The smallness holds because our interest is in the high temperature regime, which is effectively like a weak disorder assumption. Furthermore we focus on segments with range r that are larger by a comparable factor with the spatial correlation scale. For such segments one can use the estimate $\langle \exp(u) \rangle \approx \exp[(1/2) \langle u^2 \rangle]$. Longer segments can be "factorized" as in the treatment of uncorrelated field. The bottom line is that we can extract the critical field through the approximation

$$\frac{1}{2} \left\langle u^2 \right\rangle \quad \approx \quad f_c \, r \tag{23}$$

where f_c is defined as the prefactor in this linear dependence. Specifically we assume that the stochastic field is given by Eq.(17). The potential V_n is assumed to be uncorrelated, with zero average. The random variable $u = (U_{n+r} - U_n)$ is the sum $\sum \mathcal{E}_{n'}$ of correlated variables $\mathcal{E}_{n'} = \beta_{n'}[V_{n'+1} - V_{n'}]$. This can be re-arranged as a sum over uncorrelated variables. Namely, neglecting a boundary term, $u := \sum [\beta_{n'} - \beta_{n'-1}]V_{n'}$. Therefore we deduce that $\langle u^2 \rangle$ equals the number r of terms in the sum, times the variance

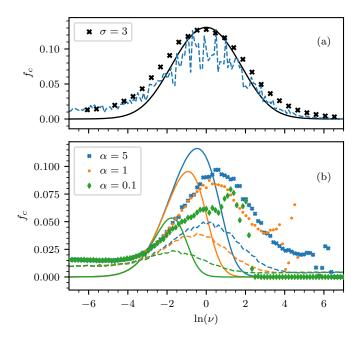


Figure 3. The threshold field f_c versus the irradiation intensity ν . The numerics is done for a ring of length L=200 with $w^{\beta}=1$. The disordered potential is with $\sigma_v=2$ and $\sigma=3$. (a) A passive particle: The analytical estimate for f_c (solid lines) is based on Eq.(24). It is compared with a numerical estimate that is based on 50 realizations using Eq.(23) with Eq.(15) (dashed lines). For the same realizations we numerically determine the average delocalization threshold (symbols). (b) An active particle: The analytical estimates for f_c (solid lines) are obtained from Eq.(24) using β_n of Eq.(53) (see text for further details and discussion). The NESS based estimates (dashed lines) are based (each) on 2000 realizations using Eq.(23) with the field of Eq.(10). Both estimates are compared with the numerically determined average delocalization threshold (symbols). The solid and dashed lines in both panels are divided by 3 as explained in Sec.(7).

 $\langle [\beta_n - \beta_{n-1}]^2 V_n^2 \rangle$ of each term. Using $\langle [\beta_n - \beta_{n+1}]^2 \rangle = 2 \text{Var}(\beta_n)$, it follows from Eq.(23) that the critical bias is

$$f_c \approx \operatorname{Var}(\beta_n) \operatorname{Var}(V_n^2)$$
 (24)

By inspection of Eq.(16), non zero $\operatorname{Var}(\beta_n)$ is implied either by random local temperature T_n , or by the presence of a driving source ν . The latter mechanism assumes that there is some bond-disorder (the bonds are not identical), or optionally a non-uniform irradiation. To obtain a concrete result, we choose (V_n/T) to be normally distributed with variance σ_v , and g_n to have a log-box distribution, $\ln(g_n) \sim [-\sigma, \sigma]$. The critical field is then

$$f_c = \frac{\sigma_v^2}{4} \left(1 - \frac{1}{\sigma^2} \log^2 \left[\frac{\cosh((s+\sigma)/2)}{\cosh((s-\sigma)/2)} \right] - \frac{2}{\sigma} \frac{\sinh(\sigma)}{\cosh(\sigma) + \cosh(s)} \right)$$
(25)

with $s \equiv \ln(\nu)$. This expression has a bell like shape, with a maximum at s = 0, for which

$$f_c = \left(1 - \frac{2}{\sigma} \tanh\left(\frac{\sigma}{2}\right)\right) \frac{\sigma_v^2}{4} \tag{26}$$

We numerically illustrate this result in Fig.3a (solid line). In this figure also the threshold field for delocalization is displayed. The latter is expected to be the same up to a factor (we further discuss this issue in Sec.(7)). Without any external field, the spectrum is real. The threshold field for delocalization is determined by the appearance of complex eigenvalues near $\lambda = 0$. The result for f_c is averaged over many realizations. We shall see later that the propulsion mechanism has effectively a similar effect as illustrated in Fig.3b.

5. Passive particle - continuum version

We consider the continuum version of the model that is sketched in Fig.1a. In this limit the derivation of f_c becomes more illuminating. The continuum version of "random walk" on a lattice is a Fokker-Planck equation that includes diffusion and drift terms:

$$\frac{\partial \rho}{\partial t} = -\frac{\partial}{\partial x} \left(v(x)\rho - D(x) \frac{\partial \rho}{\partial x} \right) \tag{27}$$

This equation can be regarded either as a stand-alone model, or as an approximation for the lattice model. In the absence of disorder the diffusion coefficient is $D_0 \equiv (1/2)(w^+ + w^-)a^2$, and the drift velocity is $v = (w^+ - w^-)a$, where a is the lattice constant (set as unity in the previous section). In the presence of disorder the drift and diffusion terms are:

$$D(x) = (1 + \nu g(x)) D_0$$
 (28)

$$v(x) = -\frac{1}{T}V'(x)D_0 \equiv -\mu_0 V'(x)$$
 (29)

where V(x) and g(x) are the continuum limit version of V_n and g_n . In complete analogy with the tight-binding version we define

$$\beta(x) \equiv \left(\frac{1}{1 + \nu g(x)}\right) \frac{1}{T} \tag{30}$$

$$\mathcal{E}(x) \equiv \frac{v(x)}{D(x)} = -\beta(x)V'(x) \equiv -U'(x)$$
(31)

The role of the lattice constant a is played by a correlation distance. We define

$$C_V(r) = \langle V(x)V(x+r)\rangle \tag{32}$$

$$C_{\beta}(r) = \langle \beta(x)\beta(x+r)\rangle - \langle \beta(x)\rangle^{2}$$
(33)

For Gaussian distribution we write

$$C_V(r) = \operatorname{Var}(V) e^{-\frac{1}{2} \left(\frac{r}{a}\right)^2} \tag{34}$$

$$C_{\beta}(r) = \operatorname{Var}(\beta) e^{-\frac{1}{2} \left(\frac{r}{a}\right)^2} \tag{35}$$

The continuum version of the Derrida formula Eq.(20), whose derivation is detailed in Appendix A, takes the form

$$v_{\text{drift}} = (1 - e^{-fL}) \left[\int_0^L dx \left\langle \frac{1}{D(x)} e^{-fx + U(x)} \right\rangle \right]^{-1}$$
(36)

In this version an ensemble average has been incorporated, and the convention U(0) = 0 is implicit.

The derivation of an expression for f_c proceeds as in the previous section. Using

$$\langle U(x)^{2} \rangle = \int_{0}^{x} \int_{0}^{x} dx_{1} dx_{2} \langle \beta(x_{1})\beta(x_{2})V'(x_{1})'V(x_{2}) \rangle$$

$$= x \int_{-\infty}^{\infty} dr \left(C_{\beta}(r) + \langle \beta(x') \rangle^{2} \right) \left(-\frac{d}{dr^{2}} C_{V}(r) \right)$$

$$= x \int_{-\infty}^{\infty} dr C_{\beta}'(r) C_{V}'(r)$$
(37)

we get

$$f_c = \frac{\sqrt{\pi}}{4a} \text{Var}(\beta) \, \text{Var}(V) \tag{38}$$

This result is consistent with Eq.(24), where we assumed Kronecker delta correlations, and lattice-constant that equals unity.

6. Active Brownian particle

We turn now to discuss the active particle system of Fig.1b. Unlike the non-Brownian version that has been discussed in the past (see Appendix B), here we have diffusion to begin with, and we ask what happens if we add propulsion. The rates of transitions are:

$$w_{(n+1)\uparrow,n\uparrow} = w_n^{\beta} e^{+\Delta_n/2T_n} + w_n^{\nu} \tag{39}$$

$$w_{n\uparrow,(n+1)\uparrow} = w_n^{\beta} e^{-\Delta_n/2T_n} \tag{40}$$

$$w_{(n+1)\downarrow,n\downarrow} = w_n^{\beta} e^{+\Delta_n/2T_n} \tag{41}$$

$$w_{n\downarrow,(n+1)\downarrow} = w_n^{\beta} e^{-\Delta_n/2T_n} + w_n^{\nu} \tag{42}$$

$$w_{n\downarrow,n\uparrow} = w_n^{\alpha} \tag{43}$$

$$w_{n\uparrow,n\downarrow} = w_n^{\alpha} \tag{44}$$

The diffusion coefficient in the absence of disorder is calculated in Appendix C. The final result is

$$D^{\text{eff}} = w^{\beta} a^2 + \frac{1}{2} w^{\nu} a^2 + \frac{[w^{\nu}]^2}{2w^{\alpha}} a^2$$
 (45)

All 3 terms in D_{eff} have a simple heuristic explanation. The last term is consistent with the continuum limit Eq.(B.2). Note that the continuum limit $(a \to 0)$ is taken such that $w^{\beta}a^2 = D$ and $w^{\nu}a = \nu$ are kept constant. Therefore the second term drops out. The first term is excluded if one considers the non-Brownian version. Once we have disorder it is convenient to define local drift velocity and local diffusion coefficient as follows:

$$v_n = \left[2 \sinh\left(\frac{\Delta_n}{2T_n}\right) \right] w_n^{\beta} a \tag{46}$$

$$D_n = \left[\cosh \left(\frac{\Delta_n}{2T_n} \right) \right] w_n^{\beta} a^2 \tag{47}$$

The zero order effect of the disorder is to replace the first term in Eq.(45) by an averaged D_n . Such zero-order treatment has no profound meaning and merely reflects our definition of w^{β} as geometric average and not as the algebraic average of the backward and forward rates.

NESS based approach.— In Appendix D we find the NESS, based on a non-Brownian approximation. Namely, we neglect counter-propulsion transitions, and assume weak disorder. Using units such that a=1 the result is

$$\frac{p_{n+1}}{p_n} \approx \left[\frac{\alpha + \nu - v_n}{\alpha + \nu + v_n} \right] \left(\frac{\nu + v_n}{\nu - v_n} \right) \tag{48}$$

Weak disorder means that the v_n are much smaller than the propulsion velocity ν . An expression for the effective \mathcal{E}_n is implied via Eq.(10). The first order expression in v_n is

$$\mathcal{E}_n \approx \frac{2\alpha v_n}{(\alpha + \nu)\nu} \tag{49}$$

Going beyond linear order but assuming small α we get a result that is consistent with the continuum limit

$$\mathcal{E}_n \approx \frac{2\alpha v_n}{\nu^2 - v_n^2} \tag{50}$$

Either way we can write $\mathcal{E}_n \equiv \beta_n v_n$, where β_n might reflect disorder that is related to α or ν . In the absence of such disorder the higher order dependence on v_n has to be taken into account. Having disordered β_n is required for the emergence of Sinai physics, as explained in previous sections.

As far as analytical estimates are concerned, the NESS based approach to obtain the stochastic field, via Eq.(10), is a dead end. Specifically, for an active Brownian particle, there is no simple way to generalized the solution such that it will take into account the counter-propulsion rates. We therefore adopt in the remaining part of this section a more flexible heuristic approach for the estimate of f_c . Numerically we compare the two methods in Fig.3. Namely, we estimate f_c from the numerically found NESS, and compare it with the heuristic analytical estimate. In the next section we highlight a somewhat more rigorous approach.

Heuristic approach.— The heuristic approach is based on the assumption that the *coarse grained* dynamics is described by a single-channel diffusion equation, namely Eq. (27). It is therefore natural to adopt continuum-limit notations. Within this framework Sinai physics emerges whenever we break locally the Einstein relation, namely,

$$\frac{\mu(x)}{D(x)} = \beta(x) = \text{disordered}$$
 (51)

Then the critical field is determined by Eq.(38). For $\nu = 0$ the local mobility μ_0 and the local diffusion coefficient D_0 are defined as in Eq.(29) and Eq.(28). More generally both may depend on x, but this dependence is not important for us because the ratio $\mu_0/D_0 = 1/T$ does not care about this dependence. For $\nu \neq 0$ the mobility is barely affected because the extra transitions do not bias the transitions. This is true for both

passive and active particles. So we can write $\mu(x) = \mu_0(x)$. But D(x) is affected. For a passive particle see Eq. (28). For an active particle we can justify the use of Eq. (45) (with an added site coordinate) provided the variation of V(x) is on large scale $a \gg \text{LatticeConstant}$. But in practice we test in Fig. 3 our formulas for uncorrelated potential (a = LatticeConstant), so inaccuracies are expected.

From the above discussion it follows that for the purpose of estimating f_c via Eq.(38) we use expression of the form

$$\beta(x) = \frac{\mu_0(x)}{D_0(x) + \nu D^{(1)}(x) + \nu^2 D^{(2)}(x)}$$
(52)

This expression with $D_0 = 0$ holds for non-Brownian particle, while for Brownian particle it is more illuminating to write it in the style of Eq.(30), namely,

$$\beta(x) = \frac{\beta_0(x)}{1 + \nu g^{(1)}(x) + \nu^2 g^{(2)}(x)}$$
(53)

where $\beta_0(x) = 1/T$ for a bath that has uniform temperature.

Smoothing effect.— In the numerics we set the units such that T = a = 1, and use Eq.(53) with the substitutions

$$g^{(1)}(x) \mapsto g_n \tag{54}$$

$$g^{(2)}(x) \mapsto \text{Smoothed}\left\{ [g_n]^2/(2\alpha) \right\}$$
 (55)

Then, f_c is calculated using Eq.(24). The results are presented in Fig.3b. If we do not perform spatial smoothing there is a rough agreement with the delocalization numerics, provided α is large, and ν is not too large. Apparently we cannot expect better because the error is comparable with the difference between the delocalization-based result and the NESS-based result. But for small values of α one observes (not displayed) a gross over-estimate: the estimated f_c becomes larger instead of getting smaller. This over-estimate can be avoided if spatial smoothing is performed. The reasoning is as follows: if α is small the mean free path is large ($\ell \sim 1/\alpha$). Therefore the effective diffusion term has to be smoothed over this scale. But alas, the smoothing procedure is analytically ill defined, and therefore in practice we were satisfied by the replacement $g^{(2)}(x) \mapsto 1/(2\alpha)$. This substitution provides a lower bound for our estimate, hence becoming an underestimate for large ν . However, for large ν there is a bigger issue that we discuss next.

Finite size effect.— We observed in Fig.3b that the f_c analytical estimate for the delocalization threshold fails for large ν . The actual threshold drops to zero at a ν value that depends on α . The failure to predict this drop cannot be attributed to its inherent limitations (those that have been pointed out in the previous paragraph). Rather some further inspection reveals that this drop of f_c is a finite-size effect. The λ_k spectrum for a non-disordered ring can be calculated analytically, see Appendix C. For a large enough ring the spectrum for f=0 is always real in the vicinity of $\lambda_0=0$. More precisely the range where it is real is restricted by the condition $\sin(k) < \alpha/\nu$. No eigenvalues reside within this range if L is too small. Accordingly, Sinai physics is observed only for $\nu < \alpha L$.

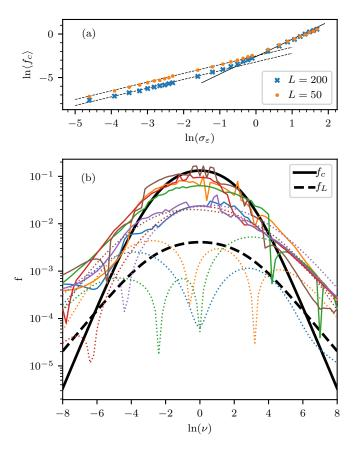


Figure 4. Demonstration of spontaneous delocalization. (a) Benchmark Sinai model: The average f_c for uncorrelated fields, for two rings with different lengths. Each symbol is the average of f_c over 300 realizations. For $f_c > f_L$, the delocalization threshold is $f_c \approx f_{1/2} \propto \sigma_\varepsilon^2$ (solid line), while for weaker bias $f_c \approx f_L \propto \sigma_\varepsilon$ (dashed lines), see Eq. (58). (b) Passive irradiated particle: We consider an $L \approx 2000$ ring with the same disorder parameters as that of Fig.3a. We plot the numerically-determined residual bias f_L (dotted lines), and delocalization threshold f_c (solid lines), for a few realizations (distinguished by color). The black thick solid and dashed lines have the same meaning as in panel (a), namely, they correspond to $f_{1/2}$ and f_L . Specifically, the black thick solid line is the same as in Fig.3a.

7. The delocalization transition

So far we have regarded the delocalization transition as a numerical trick to detect the emergence of Sinai Physics. But also from a physics-oriented perspective we have to remember that we are always dealing with a finite system, where it is meaningless to look for a sliding transition. Namely, for a finite-length ring, a non-zero f always implies a non-zero drift velocity. Thus, in the context of a finite-length ring it is appropriate to consider the delocalization transition rather than a sliding transition. We start with the benchmark Sinai model, and then apply the same reasoning for the irradiated passive particle. The same reasoning can be applies also for an active particle.

Benchmark Sinai model.— Consider a simple ring of length L, with independent stochastic fields $\mathcal{E}_n + f$, and f is defined such that $\sum_n \mathcal{E}_n = 0$, while $\text{Var}(\mathcal{E}) = \sigma_{\varepsilon}^2$. We

can also define the μ -moment f_{μ} of the random stochastic field via

$$\langle e^{-\mu\mathcal{E}}\rangle \equiv e^{-\mu f_{\mu}} \tag{56}$$

For Gaussian disorder $f_{\mu} = (\mu/2)\sigma_{\varepsilon}^2$. The bias f is regarded as a control parameter, and the relation $f = f_{\mu}$ can be inverted. Thus we can regard $\mu(f)$ as an optional way for characterization of the bias. Recall that the bias $f_c = f_1$, that corresponds to $\mu=1$, is the critical field for the sliding transition.

Delocalization threshold.— The sliding threshold f_1 concerns an ensemble average over infinite chains, while the delocalization threshold concerns a single realization of a finite size ring. The relation between the two transitions has been studies in [12] for the benchmark Sinai model. Assuming a very long ring, the threshold field for sliding is determined by a spectral density $\lambda^{\mu-1}$, where $\mu = \mu(f)$. It has been argued that the delocalization transition takes place for $\mu = 1/2$, meaning that $f_c[\text{delocalization}] \approx f_{1/2}$. For Gaussian disorder $f_{1/2} = (1/2)f_1$, while for (e.g.) a box distribution the ratio depends on σ_{ε} . However, the reasoning of [12] implicitly assumes that L is long enough, while for our purpose some further refinements are crucial.

Residual bias.— Closing a chain segment of length L into a ring, assuming uniform temperature, we get $\Phi = 0$ due to telescopic cancellations of the terms. But in the benchmark Sinai model we have an uncorrelated stochastic field, that has dispersion σ_{ε} , and therefore we get a residual affinity $\Phi \sim \sigma_{\varepsilon} \sqrt{L}$, which implies a non-zero residual bias $|f| \sim f_L$, where

$$f_L \equiv C \frac{\sigma_{\varepsilon}}{\sqrt{L}}, \qquad C \approx 0.568$$
 (57)

The numerical prefactor C is a matter of convention (see below). The residual bias f might be either positive or negative with equal probability, and one expects corresponding fluctuations of the spectral density: recall that the latter is characterized by the f-related exponent μ . Those finite size related fluctuations can be ignored if $f_{1/2} \gg f_L$, which is the implicit assumption in [12]. More generally it is natural to expect $f_c \sim f_L$ for a small ring. This expectation is confirmed by Fig.4a, where the average of $f_c(\sigma_{\varepsilon})$ for rings with two different L-s is plotted. The prefector C in the definition Eq.(57) of f_L has been determined from this figure. The conclusion can be summarized by the formula

$$f_c = \max\{f_L, \ f_{1/2}\} \sim \max\left\{\sqrt{\frac{f_{1/2}}{L}}, \ f_{1/2}\right\}$$
 (58)

From the second equality it should be obvious that the crossover takes place at $f_{1/2} \sim 1/L$. We emphasize again that for a finite-size ring f_c refers to the delocalization transition.

Irradiated ring.— Turning back to treat our irradiated ring, the $f_{1/2}$ in Eq.(58) is replaced by an estimate that is based on Eq.(24). However, we have to remember that the stochastic field \mathcal{E}_n does not have Gaussian distribution. Specifically, in our numerics, it reflects the log-normal distribution of the couplings. Thus the ratio between

 f_c [delocalization] and the f_c [sliding] estimate of Eq.(24) becomes σ dependent. For the $\sigma = 3$ data we used 1/3 in Fig.3a, and consistently the same ratio in Fig.3b.

Spontaneous delocalization.— Considering a passive particle on a ring without irradiation, and assuming uniform temperature, we get $\Phi = 0$ due to telescopic cancellations of the terms. But for $\nu \neq 0$ we expect a residual bias $f(\nu)$. The statistical properties of $f(\nu)$ has been studied in [24]. As in the benchmark Sinai model $|f(\nu)| \sim f_L$. Fig.4b illustrates this dependence for a few realizations. Indeed on the average we witness agreement with Eq.(57). We also plot there (solid line) the expected f_c for a very long ring. But we are dealing with a finite-L ring, and indeed we see that the average $f_c(\nu)$ is in agreement with Eq.(58). Based on Eq.(26), it follows that in the vicinity of $\ln(\nu) \sim 0$ we should be able to observe the emergence of Sinai physics, i.e. localization, provided

$$L \gg \frac{1}{\sigma^2 \sigma_v^2} \tag{59}$$

Along the tails we observe as expected $|f_c(\nu)| \sim f_L(\nu)$, i.e. multiple intersections of the $f_L(\nu)$ curve with the $f_c(\nu)$ curve. Thus we have, for either very weak or very strong irradiation, a sequence of spontaneous localization-delocalization transitions. As $L \to \infty$ the central Sinai region expands.

8. Discussion

Testing Sinai physics for a passive particle is possibly rather straightforward. The setup that we have considered in Eq.(12) can be literally realized as a semiconductor device. The driving source is like noise that induces extra transition between impurities.

The analogous discussion for an active particle system is somewhat motivated by experiments with Janus particle that are immersed in a solution. The propulsion can be controlled by an irradiation source. But it is not obvious whether the naive setup really leads to the emergence of Sinai physics. The model that has been introduced in [25], and the subsequent non-Brownian version that has been considered in [26, 27] assume a static disordered potential V(x) that induces a quenched velocity field $v(x) \propto -V'(x)$. This seems to be a non-physical assumption for a particle in a fluid. The question arises whether it is really feasible to perform an experiment whose objective is to witness induced sub-diffusion and a subsequent sliding transition.

Our starting point is such that for $\nu=0$ we would like to witness normal diffusion. Accordingly we refer to the Brownian version of Sec. (6). If we have in mind Janus particles, it is reasonable to assume that we can induce a uniform bias. For a charged particle it might be an electric potential $V(x) \propto -x$. This induces a nonuniform unidirectional stochastic field $\mathcal{E}(x) = -\beta(x)V'(x)$, with $\beta(x)$ that is given, say, by Eq.(53). The x dependence is not due V(x) but due to, say, the disordered irradiation. So the remaining issue is how to get control over the average bias f. In particular how do we achieve f=0. For that we need an additional mechanism that can counter-balance the average value of $\mathcal{E}(x)$. Apparently the simplest possibility is to consider a Janus particles in a flowing solution.

In the setup described above the quench disorder reflects the irradiation pattern, and the bias field is due to the net effect of having both external field and flow of the embedding fluid. Such setup allows to test the emergence of Sinai physics for an active Brownian particle.

On the theory side it was important to emphasize a few conceptual subtleties. First of all it should be clear that Sinai model concerns rigorously passive particles. Its application to active particle is not self obvious. We have elaborated several perspectives (heuristic, NESS-based, spectral-based) that support the emergence of Sinai physics for such non-equilibrium system.

We have provided estimates for the critical field $f_c(\nu)$. In practice it is Eq.(24) with $Var(\beta_n)$ of Eq.(53). We have tested our estimates numerically as in Fig.3. In order to be able to witness Sinai physics this threshold value should be non-negligible. Specifically, we have clarified how f_c is affected by a finite size effect, and consequently provided the conditions that are required in order to avoid spontaneous delocalization due to a residual bias that is induced by the irradiation source.

Appendix A. The formula for the drift velocity

The derivation of the formula for the drift velocity in the continuum limit version of Sinai model is rather simple. One notice that Eq.(27) is in essence a continuity equation for the current

$$I = -D(x)\frac{\partial \rho}{\partial x} + v(x)\rho \tag{A.1}$$

$$= -D(x)e^{-U(x)}\frac{d}{dx}\left[e^{U(x)}\rho(x)\right] \tag{A.2}$$

The steady state is obtained by solving I(x) = I = const, where I is yet unknown. One obtains

$$\rho(x) = \left[C - I \int_0^x \frac{e^{U(x')}}{D(x')} dx'\right] e^{-U(x)} \tag{A.3}$$

where the integration constant C is determined by the periodic boundary conditions $\rho_0(0) = \rho_0(L)$, namely,

$$C = \frac{I}{1 - e^{U(L)}} \int_0^L \frac{e^{U(x')}}{D(x')} dx' \tag{A.4}$$

At this point it is convenient to make the substitution U(x) := [-fx + U(x)], such that U(x) is an L-periodic function. Consequently we get

$$\rho(x) = \frac{I}{1 - e^{-fL}} \int_0^L \frac{dr}{D(x+r)} e^{U(x+r) - U(x) - fr}$$
(A.5)

From the normalization condition we get the expression for the current:

$$I = (1 - e^{fL}) \left[\int_0^L \int_0^L dx dr \frac{1}{D(x+r)} e^{U(x+r) - U(x) - fr} \right]^{-1}$$
(A.6)

Replacing the integral over x by an ensemble average, and using I = (1/L)v, we get Eq.(36).

Appendix B. Non-Brownian active particle

The passive particle that is described by the Fokker Plank Equation Eq. (27) is a Brownian particle whose motion can be described by a Langevin equation $\dot{x} = v(x) + \text{NoiseTerm}$. Without the noise D(x) = 0, which is like having a zero temperature bath. We term this noise-less case as the *non-Brownian limit*. References [26, 27] have considered this limit for an active particle, aka "run-and-tumble particle" scenario. We summarize their results in the perspective of our presentation.

The motion is described by the Langevin equation

$$\dot{x} = v(x) \pm \nu \tag{B.1}$$

where ν is the propulsion velocity, and v(x) is the velocity field. The \pm sign switches randomly with rate α . Note that in Ref[26] the switching rate is $\alpha/2$, while a different notation γ is used in [27]. In the tight binding model we use the notation w_n^{α} , and for uniform irradiation we assume $w_n^{\alpha} = \text{const} = \alpha$.

In the absence of propulsion ($\nu = 0$) we have no diffusion: we just have a transient drift due to the local v(x), which looks like having zero motion on a coarse grained scale. Turning on the propulsion and setting v(x) = 0 the coarse grained dynamics of the probability density $\rho(x)$ becomes diffusive with

$$D^{\text{eff}} = \frac{\nu^2}{2\alpha} \tag{B.2}$$

This effective diffusion is due to the interplay between the propulsion (motion with velocity $\pm \nu$) and the random changes in the orientation of the particle (with rate α). In the presence of v(x) one obtains a quasi-canonical NESS [26]:

$$\rho(x) \propto \frac{\nu}{\nu^2 - v(x)^2} \exp\left[-U(x)\right] \tag{B.3}$$

Here U(x) is the effective stochastic potential that is associated with with an effective stochastic field

$$\mathcal{E}(x)^{\text{eff}} = \frac{2\alpha v(x)}{\nu^2 - v(x)^2} \tag{B.4}$$

In leading order with respect to v(x), the result is $\mathcal{E}(x) = v(x)/D_0$. We have $v(x) \propto -V'(x)$ and therefore $U(x) \propto V(x)$ is bounded, which implies that Sinai physics does not emerge. But if we go beyond leading order, and take the appearance of v(x) in the denominator of Eq.(B.4) into account, then the telescopic correlations are broken, U(x) becomes unbounded, and Sinai physics emerges. An optional way to break the telescopic correlations is to assume randomness in α or in ν .

Appendix C. Diffusion of active particles

Here we write again the rates of Sec. (6) with simplified notation

$$w_{(n+1)\uparrow,n\uparrow} = D_n + \frac{v_n}{2} + \nu \tag{C.1}$$

$$w_{n\uparrow,(n+1)\uparrow} = D_n - \frac{v_n}{2} \tag{C.2}$$

$$w_{(n+1)\downarrow,n\downarrow} = D_n + \frac{v_n}{2} \tag{C.3}$$

$$w_{n\downarrow,(n+1)\downarrow} = D_n - \frac{v_n}{2} + \nu \tag{C.4}$$

$$w_{n\downarrow,n\uparrow} = \alpha$$
 (C.5)

$$w_{n\uparrow,n\downarrow} = \alpha$$
 (C.6)

In the absence of disorder we set $D_n = D_0$ and $v_n = v_0$. The calculation of the effective diffusion coefficient, is done with the help of Bloch theorem. In the momentum basis, the rate matrix is block diagonal in k. The blocks are

$$\mathbf{W}^{(k)} = \begin{pmatrix} A_{+}^{(k)} - A_{+}^{(0)} - \alpha & \alpha \\ \alpha & A_{-}^{(k)} - A_{-}^{(0)} - \alpha \end{pmatrix}$$
(C.7)

where

$$A_{\pm}^{(k)} = 2D_0 \cos(k) - iv_0 \sin(k) + \nu e^{\mp ik}$$

The eigenvalues are denoted $-\lambda_{k,\pm}$. The drift velocity and diffusion coefficient are found by expanding $\lambda_{k,+}$ as in Eq.(11). The drift velocity comes out v_0 as expected, and for the diffusion coefficient we get

$$D^{\text{eff}} = D_0 + \frac{\nu}{2} + \frac{\nu^2}{2\alpha} \tag{C.8}$$

In terms of the parameters that are used in the main text, we get Eq.(45).

For completeness we write the explicit expression for the eigenvalues. In the absence of bias this expression is rather simple:

$$\lambda_{k,\pm} = -\left[c \pm \sqrt{\alpha^2 - a^2}\right] \tag{C.9}$$

with

$$\alpha = w^{\alpha}$$

$$a = w^{\nu} \sin(k)$$

$$c = (2w^{\beta} + w^{\nu}) \cos(k) - \left[w^{\alpha} + (2w^{\beta} + w^{\nu})\right]$$

For $w^{\nu} > w^{\alpha}$ some of the eigenvalues become complex, but the small k eigenvalues at the vicinity of $\lambda = 0$ are always real. The latter statement assumes a very long ring. For a finite ring of length L such eigenvalues (with $k \sim 1/L$) exist provided w^{ν} is smaller compared with $w^{\alpha}L$.

Band mixing.— The essence of Sinai physics is that weak bias is not able to make the spectrum complex, as opposed to the non disordered result Eq. (11). Instead, f has to exceed a threshold to make the spectrum complex. It is important to remember that we care here about the spectrum at the vicinity of $\lambda = 0$. The above perspective applies also for an active particle. Namely, also for an active particle in a disordered environment the spectrum at the vicinity of $\lambda = 0$ remains real if f is small enough. This observation is based on the following reasoning. The diagonalization of W = H + Acan be treated within the framework of perturbation theory as explained in Section V of [25]. Here H is a real symmetric matrix, while A is a real anti-symmetric matrix. It is well known (usually in the context of PT-symmetric non-hermitian Hamiltonians) that in order to get complex spectrum the elements of A should be large enough in the sense of perturbation theory (the coupling should be larger than the "energy-difference" of the coupled states), else the spectrum remains real. In the present context H is composed of two uncoupled \pm blocks, while $A = A_{\perp} + A_{\parallel}$ is composed of propulsionrelated-perturbation and bias-related-perturbation, respectively. The former induces inter-band coupling, while the latter induces intra-band couplings. Without A_{\perp} we have the standard delocalization scenario: if the intra-band non-hermitian perturbation is strong enough one observes Sinai-type delocalization (complex eigenvalues). On the other hand, without A_{\parallel} , we have only inter-band couplings that are likely to induce complexity only in the band-overlap region. This argument assumes that the propulsion is not too extreme, such that we stay within the Sinai regime. In other words: we can establish the emergence of Sinai physics for active particles, but we cannot exclude the existence of additional regimes.

Appendix D. NESS for non-Brownian active particle

The NESS can be easily found for a unidirectional stochastic motion. The propulsion rate ν is modulated by the velocity field of the disordered bath, and the counterpropulsion rates are neglected. Instead of the rates as written in 6 we use the following non-Brownian version:

$$w_{(n+1)\uparrow,n\uparrow} = \nu + v_n \equiv w_n^+ \tag{D.1}$$

$$w_{n\uparrow,(n+1)\uparrow} = 0 \tag{D.2}$$

$$w_{(n+1)\downarrow,n\downarrow} = 0 \tag{D.3}$$

$$w_{n\downarrow,(n+1)\downarrow} = \nu - v_n \equiv w_n^- \tag{D.4}$$

$$w_{n\downarrow,n\uparrow} = \alpha$$
 (D.5)

$$w_{n\uparrow,n\downarrow} = \alpha$$
 (D.6)

One can verify that for a non-disordered system the diffusion coefficient is the same, namely Eq.(C.8), but without the first term.

The NESS is determined by the equation $\boldsymbol{W}\boldsymbol{p}=0$. In the Sinai regime the drift velocity vanishes. Formally this statement is exact only in a statistical sense (for an infinite chain). Consequently, for a very long ring we expect an exponentially small NESS

current. Below we find the zero-current solution. It can be regarded as an approximation for the exact NESS. Clearly we are using here a self-consistent approximation scheme: outside of the Sinai regime this scheme fails. The extreme illustration for the failure of this procedure is the case of a non-disordered ring (in the continuum limit it is Eq.(27) with constant D and v). The zero current solution for non-zero v is exponentially diverging in one direction, and cannot be matched if one tries to impose periodic boundary conditions. The true NESS in the latter case does not feature an exponentially small current.

The equation for the zero-current NESS for non-Brownian active particle is

$$p_{n+1,\downarrow} = \left(\frac{w_n^+}{w_n^-}\right) p_{n,\uparrow} \tag{D.7}$$

From the Kirchhoff equation at node $(n+1,\uparrow)$ we deduce that

$$\frac{p_{n+1,\uparrow}}{p_{n,\uparrow}} = \left[\frac{\alpha + w_n^-}{\alpha + w_{n+1}^+}\right] \left(\frac{w_n^+}{w_n^-}\right) \tag{D.8}$$

From here it follows that

$$\frac{p_{n+1}}{p_n} = \frac{\left[1 + \frac{\alpha + w_n^-}{\alpha + w_{n+1}^+}\right]}{\left[1 + \frac{\alpha + w_n^+}{\alpha + w_{n-1}^-}\right]} \left(\frac{w_n^+}{w_n^-}\right)$$
(D.9)

The effective stochastic field is found via Eq.(10).

Acknowledgment.— This research was supported by the Israel Science Foundation (Grant No.283/18).

- [1] Sinai Y G 1982 Theory of Probability & Its Applications 27 256–268 [link]
- [2] Derrida B 1983 Journal of Statistical Physics 31 433–450 ISSN 1572-9613 [link]
- [3] Bouchaud J P, Comtet A, Georges A and Le Doussal P 1990 Annals of Physics 201 285–341 [link]
- [4] Bouchaud J P and Georges A 1990 Physics Reports 195 127 293 [link]
- [5] Le Doussal P and Vinokur V M 1995 Physica C: Superconductivity 254 63–68 [link]
- [6] Hatano N and Nelson D R 1996 Phys. Rev. Lett. 77(3) 570–573 [link]
- [7] Hatano N and Nelson D R 1997 Phys. Rev. B **56**(14) 8651–8673 [link]
- [8] Shnerb N M and Nelson D R 1998 Physical review letters 80 5172 [link]
- [9] Feinberg J and Zee A 1999 Phys. Rev. E **59**(6) 6433–6443 [link]
- [10] Kafri Y, Lubensky D K and Nelson D R 2004 Biophysical Journal 86 3373 3391 [link]
- [11] Kafri Y, Lubensky D K and Nelson D R 2005 Phys. Rev. E 71(4) 041906 [link]
- [12] Hurowitz D and Cohen D 2016 Scientific reports 6 [link]
- [13] Hurowitz D and Cohen D 2016 Phys. Rev. E 93(6) 062143 [link]
- [14] Stein D L and Newman C M 1995 Physical Review E 51 5228 [link]
- [15] Reichhardt C and Reichhardt C O 2014 Physical Review E 90 012701 [link]
- [16] Reichhardt C O and Reichhardt C 2018 New Journal of Physics 20 025002 [link]
- [17] Reichhardt C and Reichhardt C J O 2017 Journal of Physics: Condensed Matter 30 015404 [link]
- [18] Reichhardt C and Reichhardt C J O 2021 Physical Review E 103 062603 [link]
- [19] Bertrand T, Zhao Y, Bénichou O, Tailleur J and Voituriez R 2018 Physical Review Letters 120 198103 [link]
- [20] Walther A and Müller A H E 2013 Chemical reviews 113 5194–5261 [link]
- [21] Wheat P M, Marine N A, Moran J L and Posner J D 2010 Langmuir 26 13052–13055 [link]
- [22] Menzel A M 2015 Physics reports **554** 1–45 [link]
- [23] Maggi C, Simmchen J, Saglimbeni F, Katuri J, Dipalo M, Angelis F D, Sanchez S and Leonardo R D 2015 Small 12 446–451 [link]
- [24] Hurowitz D, Rahav S and Cohen D 2013 Physical Review E 88 062141 [link]
- [25] Shapira D, Meidan D and Cohen D 2018 Phys. Rev. E 98(1) 012107 [link]
- [26] Dor Y B, Woillez E, Kafri Y, Kardar M and Solon A P 2019 Physical Review E 100 052610 [link]
- [27] Le Doussal P, Majumdar S N and Schehr G 2020 EPL (Europhysics Letters) 130 40002 [link]
- [28] Hänggi P and Marchesoni F 2009 Reviews of Modern Physics 81 387 [link]